

A re-examination of the interstitial Ti levels in Si

Vladimir Kolkovsky*, Leopold Scheffler, and Joerg Weber

Technische Universität Dresden, 01062 Dresden, Germany

Received 4 May 2012, revised 25 May 2012, accepted 25 May 2012

Published online 16 August 2012

Keywords Si, Ti, DLTS, interstitial

* Corresponding author: e-mail kolkov@ifpan.edu.pl, Phone: +049 351 463 38688, Fax: +049 351 463 37060

Using high-resolution Laplace DLTS studies we demonstrate that three Ti-related levels (E40, E150 and H180) previously assigned to the different charge states of the interstitial Ti belong to different Ti defects. The enhancement of the emission rates of E40 and H180 as a function of the electric field (Poole-Frenkel effect) shows that these defects are charged before they capture a majority carrier in n- and p-type Si, respectively. In contrast

to the previous studies we did not observe the Poole-Frenkel effect for E150. The inconsistency is correlated with the presence of H-related defects close to E150, which cannot be distinguished by using the conventional DLTS technique. The absence of the Poole-Frenkel effect for E150 indicates that the defect is an acceptor in n-type Si. The origin of the defects will be discussed.

© 2012 WILEY-VCH Verlag GmbH & Co. KGaA, Weinheim

1 Introduction Basic studies of transition metal (TM) impurities in Si have received growing interest in recent years. The reason is their technological importance in the field of photovoltaic and Si-based integrated circuits. The TM impurities can be easily introduced during various processing steps and often they are associated with strong recombination centers [1–4]. Ti is one of the slowest diffusers which makes it very difficult to getter [5]. In addition Ti severely degrades p-base Si solar cells and therefore it acts as a lifetime killer in Si [5]. However, the electrical properties of Ti-related defects are still not well understood.

Usually three Ti-related levels were observed in the Si band gap. Two of them were assigned to the single acceptor and single donor states and they are located in the upper part of the band gap around $E_C - 0.1$ eV (E40) and $E_C - 0.27$ eV (E150) below the conduction band, respectively [6–8]. The third level which was believed to be the double donor is introduced in the lower part of Si band gap at around $E_V + 0.24$ eV (H180) above the valence band [8]. Previously, all the defects were assigned to isolated interstitial Ti. However the findings are not consistent with the results of *ab initio* molecular-dynamics simulations. Backlund *et al.* [9] reported that the acceptor level of interstitial Ti should be buried in the conduction band whereas two donor levels of interstitial Ti should be observed in n- and p-type Si, re-

spectively. In addition, the authors suggested that substitutional Ti should introduce two levels into the band gap of Si. The single acceptor level is close to the conduction band whereas the single donor level should be located just above the valence band. The co-existence of substitutional and interstitial Ti was also recently confirmed by Rutherford backscattering spectroscopy (RBS) and channeling-RBS measurements in Ti-implanted n-type Si [10]. However, no substitutional Ti-related levels were identified by means of the conventional DLTS technique.

One should also notice that in *as-grown* samples the Ti donor level (E150) was frequently reported to show a weak Poole-Frenkel effect. Usually the enhancement of the emission rate of a carrier from the defect as a function of the electric field [11] appears for charged defects before they capture a carrier while it should not be observed for defects which are neutral. However, the enhancement for carriers from E150 was significantly smaller than expected for the Poole-Frenkel effect [12,13].

In the present study we analyze Ti-related defects in Fz- and Cz-grown Si with application of the high-resolution Laplace Deep Level Transient Spectroscopy (Laplace DLTS). We demonstrate that dominant peaks in n-type Si consist of two and more peaks which cannot be separated properly by means of the conventional DLTS technique. The presence of the minor defects influences the

electrical properties of the Ti-related defects and therefore it can result in misleading conclusions.

2 Experimental Samples were cut from Ti melt doped single crystalline silicon grown by the Czochralski (CZ) or by the float-zone (FZ) technique. Phosphorus was used for *n*-type and boron for *p*-type doping. The shallow doping concentrations were $\sim 1 \times 10^{14} \text{ cm}^{-3}$ and $1 \times 10^{15} \text{ cm}^{-3}$ in *n*-type and *p*-type, respectively. Schottky contacts with the area of 0.8 and 1 mm² were formed by evaporation of aluminum for *p*-type and gold for *n*-type samples through a metal mask at room temperature. An eutectic InGa alloy is rubbed onto the back side of the samples to form the Ohmic contact. Before the contact evaporation the samples were dipped in a 1:2 mixture of HF and HNO₃ for 10–120 seconds. Also some samples were wet chemically etched with CP4a solution (HF:HNO₃:CH₃COOH in a ratio of 3:5:3). The quality of the Schottky contacts was confirmed by current-voltage measurements performed at room temperature.

The shallow dopant profiles were determined by CV measurements performed at 1 MHz. DLTS and high-resolution Laplace DLTS measurements were performed to investigate the electrical properties of deep levels in the band gap. The peak labeling used corresponds to that reported in Ref. [12]. The Poole-Frenkel effect was measured by varying the reverse bias of the diode whereas two filling pulses were kept constant with $V_{p1} = 0 \text{ V}$ and $V_{p2} = -1 \text{ V}$, respectively.

3 Experimental results and discussion Figure 1 shows a typical DLTS spectrum recorded with a reverse bias of -2 V and a filling pulse of 0 V in *p*-type (a) and *n*-type (b) Si doped with Ti. As seen in the figure two dominant peaks (E40 and E150) were observed in *n*-type Si whereas one peak labelled H180 was detected in *p*-type Si. As mentioned above, the peaks were previously correlated with the single acceptor, single donor and double donor states of interstitial Ti. One should notice that in the samples with higher H content a peak at around 260 K (E260) can be also observed in *n*-type Si. The peak was previously assigned to a TiH defect [13].

Figure 2 shows Laplace DLTS spectra recorded at different temperatures in *n*- and *p*-type Si. In good agreement with the conventional DLTS spectra three dominant peaks were also observed in the Laplace DLTS spectra. However, besides the dominant defects some minor peaks were resolved using the Laplace DLTS technique. These peaks were observed only when the probed region was chosen close to the surface. The intensity of the minor peaks depends significantly on the duration of the wet chemical etching with CP4 or CP4a solutions. With an increase of the etching time the concentration of the defects corresponding to the weak peaks increases. In addition the minor peaks were not observed in the 300 °C annealed samples. Some of the minor levels were previously observed in

Ref. [13]. Jost *et al.* reported that different TiH-related complexes could be formed in Ti-doped Si after wet chemical etching. The TiH-related defects anneal out at temperatures above 200 °C. Due to the different concentrations of the defects corresponding to the minor peaks we conclude them to belong to different defects. Tentatively, we correlate E40', E170, E170' and E260 with TiH-complexes which probably contain different number of H atoms. The assignment is consistent with the higher concentration of the defects near the surface. However, further studies are necessary to understand the origin of the defects. Also it is interesting to note that no H-related peaks were observed in *p*-type Si. The absence of TiH-related defects is believed due to the Coulombic repulsion between the positive charged H and interstitial Ti which makes it impossible to pair them up.

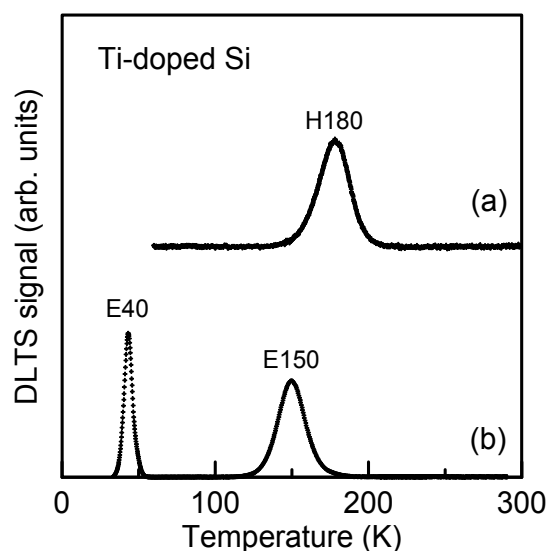


Figure 1 DLTS spectra of (a) *p*- and (b) *n*-type Si doped with Ti. The DLTS spectra were recorded with the following parameters: $V_R = -2 \text{ V}$, $V_p = 0 \text{ V}$, $t_p = 1 \text{ ms}$, and $e_n = 50 \text{ s}^{-1}$

Table 1 combines the electrical properties of the peaks (activation enthalpy and apparent capture cross section) and their possible assignment. In order to reveal the charge state of the dominant defects we investigate the dependence of the emission rates on the electric field in the depletion layer of the diode.

Figure 3 shows Laplace DLTS spectra recorded at 165 K with a reverse bias of -9 and -3 V while the filling pulses were kept constant at 0 and -1 V, respectively. Varying the reverse bias we change the electric field in our sample. As mentioned above the larger electric field should enhance the emission of carriers from donor-like defects in *n*-type Si and from acceptor-like defects in *p*-type Si. In contrast, the emission rate of a neutral defect before it captures a carrier should not be influenced by the electric field changes.

As shown in Fig. 3 the emission rate of E150 does not depend on the electric field whereas those of E170 and E170' are increased by the higher electric field. The presence of the H-related defects can explain the weak shift of the conventional DLTS peak at 150 K frequently observed by different groups [11,12]. When more hydrogen is introduced into the sample the intensity of the minor peaks becomes larger. The higher electric field shifts the minor peaks towards higher emission rates in the Laplace DLTS spectrum and towards lower temperatures in the conventional DLTS spectrum. Then the shift of E170 and E170' results in the shift of the maximum of the DLTS peak E150 which is the superposition of E150, E170 and E170'. Therefore, the observed shift of E170 and E170' was often wrongly interpreted as a weak Poole-Frenkel effect of E150.

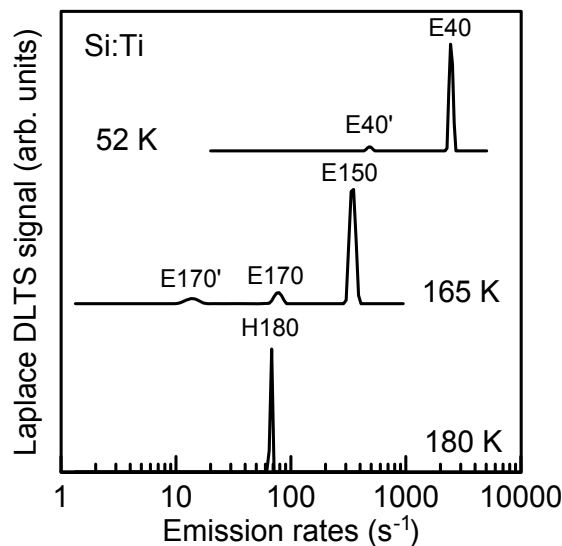


Figure 2 Laplace DLTS spectra of p- and n-type Si doped with Ti.

In contrast to E150, E40 and H180 demonstrate the enhancement of the emission rates as a function of the square root of the electric field. Figure 4 shows the dependence of the emission rates of the defects on the electric field recorded at 52 K and 180 K in n-type and p-type Si, respectively. The solid lines fit the experimental points according to the following equation [11]:

$$e_n^{PF} = e_{n0} \cdot \exp\left(\frac{\Delta E^{PF}}{k_B T}\right) = e_{n0} \cdot \exp\left(\frac{\alpha_{PF} \sqrt{F}}{k_B T}\right), \quad (1)$$

where $\alpha_{PF} = q \sqrt{\frac{Zq}{\pi \epsilon_0 \epsilon_r}}$ according to the Hartke model

(three-dimensional Poole-Frenkel effect). (2)

k_B is the Boltzmann constant, q is the elementary charge, ϵ_r is the dielectric constant, ϵ_0 is the free-space permittivity, Z is the charge state of the defect, and ΔE^{PF} is the barrier lowering due to the electric field F .

From the fitting of the experimental data $\alpha_{PF}/(kT)$ was found to be 0.0053 (using Eq. (2) it should be 0.0057) and 0.0006 (using Eq. (2) it should be 0.0014) for E40 and H180, respectively. The obtained coefficient α_{PF} for E40 is in good agreement with the single donor state of the defect whereas it is a factor of 2 smaller for H180 in comparison to that predicted for the double donor state of Ti. The smaller coefficient of H180 can be explained taking into account the electron capture barrier of the defect (about 0.045 eV) as reported in Ref. [14]. The presence of the capture barrier can significantly suppress the Poole-Frenkel effect and therefore the enhancement of the emission rate of a defect is smaller in comparison to that expected in the frame of the Hartke model. Similarly, the

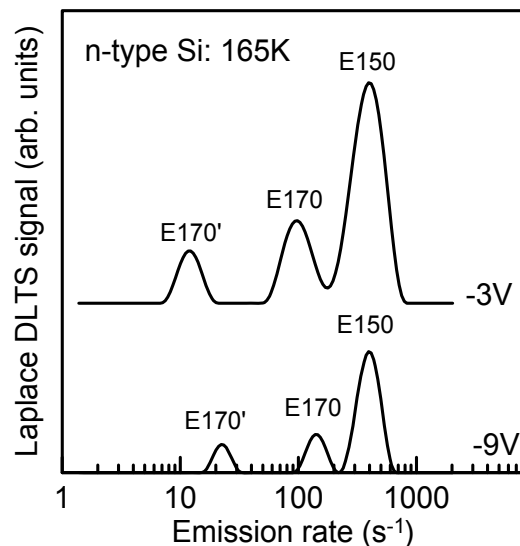


Figure 3 Laplace DLTS spectra of n-type Si recorded with different values of the reverse bias. The two filling pulses were constant 0 V and -1 V in both cases.

single donor state of the EL2 defect has never shown the Poole-Frenkel effect in *n*-type GaAs due to the large barrier for the capture of electrons [15].

As follows from the obtained results the three levels previously assigned to the single acceptor, single donor and double donor states of interstitial Ti belong to two different defects. Indeed, the Poole-Frenkel effect observed for E40 shows that the defect is a single donor whereas the absence of the field-effect for E150 assigns the defect to an acceptor. According to the *ab-initio* calculations the interstitial Ti should have a positive-*U* sequence of the levels in the band gap of Si [9]. The positive-*U* system means that the second carrier on the defect should be the more loosely bound than the first one and therefore, the acceptor level

should be located closer to the conduction band than the donor level. Then it is very likely that E40 and E150 originate from two different defects, since here the order of acceptor and donor level is reversed. We tentatively assign the E40 and H180 defects to the single donor and double donor states of interstitial Ti whereas E150 is probably the single acceptor state of substitutional Ti. However, further studies are necessary to understand the origin of the defects.

Table 1 The activation enthalpy, apparent capture cross section and possible assignment of the defects observed in Figs. 1 and 2. The activation enthalpy is given in meV from the bottom of the conduction band or from the top of the valence band.

Defects	Activation enthalpy, meV	Apparent capture cross section, cm ²	Assignment
E40	80	3×10^{-14}	Ti ("Ti _i ")
E40'	80	3×10^{-14}	TiH-related
E150	270	3×10^{-15}	Ti ("Ti _s ")
E170'	380	1×10^{-13}	TiH-related
E170	340	4×10^{-14}	TiH-related
H180	180	5×10^{-16}	Ti ("Ti _i ")

4 Conclusions In the present study we showed that three Ti-related defects previously assigned to single acceptor, single donor and double donor states of interstitial Ti belong to different defects. In addition three TiH-related levels were observed in the upper-half of the Si band gap. Different concentrations of the TiH-related defects suggest different structures of the defects. However, further studies are necessary to understand the origin of the peaks. No TiH peaks were observed in the lower part of the band gap.

Acknowledgements We acknowledge Frau S. Behrendt for the help in the sample preparation. The specially prepared samples were supplied by IKZ Berlin and Siltronic AG. Part of this work was supported by the German Ministry for Education and Research under contract 03SF0398K (xμ – Material) in the framework of the Excellence Cluster Solar Valley Central Germany.

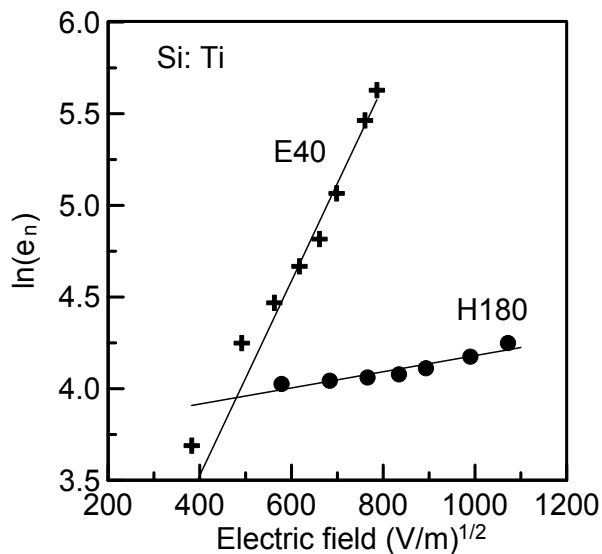


Figure 4 The field dependence of the emission rates of E40 and H180. The solid lines fit the experimental data with Eq. (1).

References

- [1] A. A. Istratov, H. Hieslmair, and E. R. Weber, *Appl. Phys. A: Mater. Sci. Process.* **70**, 489 (2000).
- [2] E. R. Weber, *Appl. Phys. A* **30**, 1 (1983).
- [3] J.-U. Sachse, J. Weber, and E.O. Sveinbjornsson, *Phys. Rev. B* **60**, 1474 (1999).
- [4] V. Kolkovsky, O. Andersen, L. Dobaczewski, A. R. Peaker, and K. B. Nielsen, *Phys. Rev B* **73**, 195209 (2006).
- [5] A. Rohatgi, J. R. Davis, R. H. Hopkins, P. Rai-Choudhury, and P. G. McMullin, *Solid-State Electron.* **23**, 415 (1980).
- [6] L. C. Kimerling, J. L. Benton, and J. J. Rubin, *Inst. Phys. Conf. Ser.* **59**, 217 (1980).
- [7] K. Graf and H. Pieper, in: *Semiconductor Silicon*, edited by H. R. Huff, R. J. Kriegler, and Y. Takeishi (The Electrochemical Society, Pennington, NJ, 1981), p. 331.
- [8] J. W. Chen, A. G. Milnes, and A. Rohatgi, *Solid-State Electron.* **22**, 801 (1979).
- [9] D. J. Backlund and S. K. Estreicher, *Phys. Rev. B* **82**, 155208 (2010).
- [10] J. Olea, M. Toledano-Luque, D. Pastor, G. Gonzalez-Diaz, and I. Martil, *J. Appl. Phys.* **104**, 016105 (2008).
- [11] S. D. Ganichev, E. Ziemann, W. Prettl, I. N. Yassievich, A. A. Istratov, and E. R. Weber, *Phys. Rev B* **61**, 10361 (2000).
- [12] D. Mathiot and S. Hocine, *J. Appl. Phys.* **66**, 5862 (1989).
- [13] W. Jost and J. Weber, *Phys. Rev. B* **54**, R11038 (1996).
- [14] S. Kuge and H. Nakashima, *Jpn. J. Appl. Phys.* **30**, 2659 (1991).
- [15] W. R. Buchwald and N. M. Johnson, *J. Appl. Phys.* **64**, 958 (1998).